Adsorption of hexavalent chromium from aqueous solution onto corn cobs – activated carbon

Pinar Bozbeyoglu[1] (iD), Ali Gundogdu[2]* (iD)

[1] Gümüşhane University, Gümüşhane Vocational School, Department of Electronics and Automation, Biomedical Device Technology Program, 29100, Gümüşhane, Türkiye

[2] Karadeniz Technical University, Maçka Vocational School, Department of Pharmacy Services, 61750, Trabzon, Türkiye

Abstract

This study evaluated the performance of a new activated carbon (CCs-AC) produced from corn cobs by boric acid activation for the effective removal of hexavalent chromium, a heavy metal with high potential to pollute the environment, from wastewater. For this purpose, with the help of parameters such as solution pH, contact time, initial Cr(VI) concentration, CCs-AC dose, desorption, and temperature, the removal of Cr(VI) ions from aqueous solution by adsorption onto CCs-AC was investigated using equilibrium, kinetic, and thermodynamic approaches. As a result of the experiments, it was determined that the optimum solution pH was 2.0, the contact time was 4 hours, and the desorption solution was 3.0 M NaOH. From the kinetic data, it was determined that the adsorption was compatible with the pseudo-second order kinetic model. The maximum Cr(VI) adsorption capacity of 123.7 mg/g obtained from the Langmuir isotherm model showed that CCs-AC was competitive with the literature. R_L values between 0.42–0.03 indicated that Cr(VI) adsorption on CCs-AC was favorable. From the thermodynamic data, the ΔH value of 12.00 kJ/mol indicated that the adsorption was rather chemically driven, while the positive value indicated that the adsorption was endothermic. Negative ΔG values indicate that Cr(VI) adsorption occurs spontaneously with increasing temperature, while the ΔS value is interpreted as an increase in the amount of unused energy.

Keywords: Adsorption, corn cobs – activated carbon, equilibrium, hexavalent chromium, kinetics, thermodynamics

1. Introduction

Chromium is known as one of the most common and most hazardous toxic heavy metals in industrial wastewater. Chromium is widely used in various industrial applications such as leather tanning, batteries, steel metallurgy, petroleum refining, paint manufacturing, electroplating, and textile industry. The most stable known forms of chromium are the trivalent and hexavalent forms [1]. The hexavalent form of chromium, Cr(VI), is much more toxic than the trivalent form, Cr(III), and both forms are highly soluble in water. Especially in bodies exposed to Cr(VI), it can accumulate in the liver, kidneys and stomach and cause many bad diseases, including cancer [2]. The limit value for total chromium species reported by the World Health Organization (WHO) in 2017 under the title "Guidelines for drinking water quality" is 0.05 mg/L [3]. Therefore, it is vital to eliminate Cr(VI) as well as various pollutant species from industrial wastewater and to release these waters to nature after treatment in a way that does not cause health problems.

Various physicochemical and electrochemical methods have been developed to reduce heavy metal concentrations in wastewater to acceptable limits. Adsorption, membrane filtration, chemical precipitation, ion exchange, photocatalysis, electrodialysis, and nanotechnology, which has been developed in recent years, are some of the methods used to remove metal ions from aqueous media. Adsorption is the process of attaching a species, called adsorbate, to the surface of another material, called adsorbent [2]. For this purpose, activated carbon, which exhibits unique properties with its porosity, large surface area and rich functional groups in its active sites, ranks first among the preferences [4]. Due to these unique properties of activated carbon and its high performance in removing pollutants from water, its commercial production from various materials such as coal, wood, fruit seed shells, coconut shells, nut shells and polymer-based synthetic raw materials with high carbon content has become very common [5]. However, due to the high cost of

commercial activated carbons, studies on the production of much lower cost and high-performance activated carbon from agricultural wastes or by-products are increasing day by day [6]. For example, many agricultural wastes such as apricot stones [7], cherry stones [8], palm oil stones [9], olive stones [10], grape seeds [11], almond shells [12], nut shells [13], corn cobs [14], rice husks [15], and sugarcane bagasse [16] have been used to produce activated carbon [17].

In today's technology, activated carbon is mainly produced by two methods: (*i*) chemical activation method using mineral acids, bases, or salts (such as HCl, NaOH, and $ZnCl_2$) as activating agents, and (*ii*) physical activation method using steam or CO_2 as activating agents. In chemical activation, the precursor (the starting material) is first impregnated with the activating agent and then subjected to carbonization in an N_2 atmosphere at temperatures in the range 400–1000 °C. In physical activation, activation and carbonization are carried out simultaneously. It requires carbonization of the precursor at temperatures above 700 °C followed by gasification in CO_2, steam, or a mixture thereof [18].

In this study, a new activated carbon was produced by chemical activation using boric acid from corn cobs as a precursor. When the literature is reviewed, it is observed that activated carbons with different properties have been produced from corn cobs using many activating agents, but the use of boric acid as a chemical activating agent is found in only one study and that study belongs to our group. In that study, the adsorption mechanisms of Cd metal and methylene blue on the activated carbon were investigated [19]. In this study, the main objective was to investigate the adsorption performance of the produced activated carbon for the removal of Cr(VI) ions from aqueous media by equilibrium, kinetic and thermodynamic parameters. Therefore, from this point of view, this study is also original.

2. Materials and methods

2.1. Preparation, production, and characterization of CCs-AC
Corn cobs (CCs) were obtained from corns collected from agricultural fields in Akçaabat district of Trabzon, Türkiye. CCs were washed thoroughly with tap water, rinsed with distilled water and dried in an oven at 105 °C for 24 hours after being left outdoors for 3 days. The dried CCs were ground in a knife grinder and sieved to a size of approximately 4–8 mm. 60 g CCs and 60 g boric acid (H_3BO_3) were mixed in 700 mL distilled/deionized water. The resulting mixture was converted into activated carbon by pyrolysis at 700 °C in N_2 atmosphere as detailed in the literature and labeled as CCs-AC (corn cobs – activated carbon) [19].

As reported in the literature, CCs-AC produced by boric acid activation was characterized by many parameters such as proximate-ultimate analysis, Boehm titration, pH-pHpzc determination, SEM images (Fig. 1), IR spectra and surface characterization analysis [19].

Fig. 1 shows SEM images of the original CCs and CCs-AC produced at 700 °C in N_2 atmosphere. Although there are roughnesses, indentations and protrusions in the structure of CCs, no porosity is visible. Activating agents such as boric acid act to dehydrate the structure at high temperatures in N_2 atmosphere and causing the formation of fractures, voids, channels, indentations, and protrusions and thus pores of a different character. This porosity of activated carbons, as well as the functional groups in the reorganized active sites on their surfaces, play a major role in making them unique adsorbents [20].

2.2. Adsorption tests
14.14 g $K_2Cr_2O_7$ (Merck, Darmstadt, Germany) was weighed, dissolved in distilled/deionized water and diluted to 1 L to prepare 5000 mg/L of a stock Cr(VI)
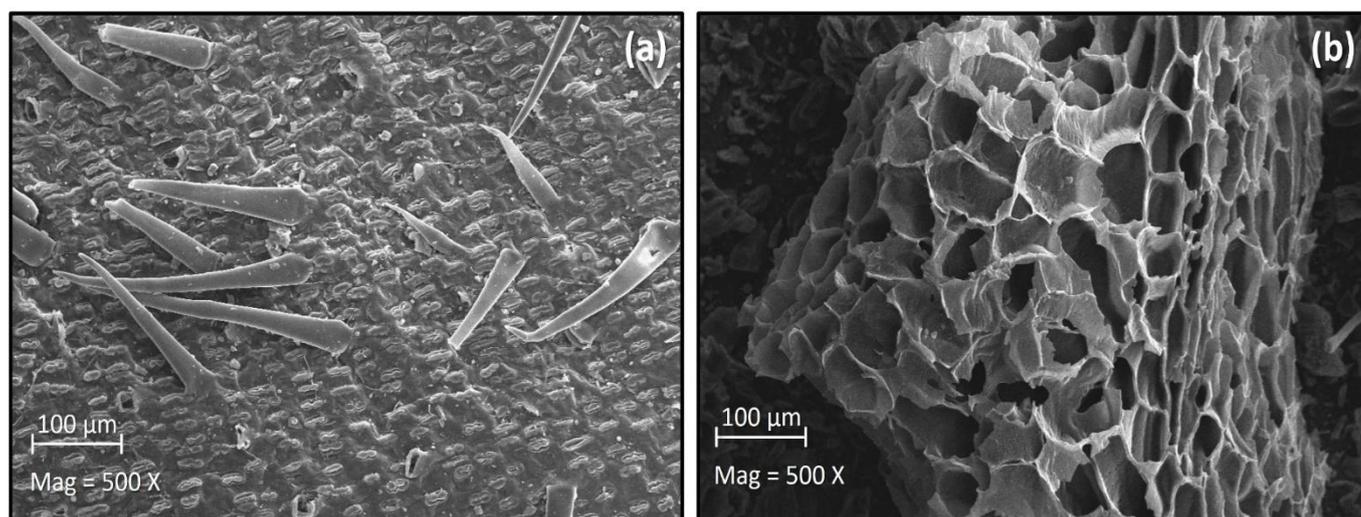
Figure 1. SEM images for (a) Corn cobs (CCs) and (b) Corn cobs – activated carbon (CCs-AC)

solution. The stock Cr(VI) solution was diluted in appropriate ratios and used in adsorption tests. Cr(VI) adsorption tests were carried out in batch mode.

10 mL of the solution prepared by diluting 5000 mg/L Cr(VI) stock solution to the desired ratio and 0.05 g of CCs-AC ground to ≤ 125 μm particle size were mixed in a polypropylene falcon tube of 15 mL volume (5.0 g/L suspension). The resulting mixture was shaken on a mechanical shaker for 4 hours. The solid-liquid mixture was separated by vacuum filtration and the concentration of Cr(VI) remaining unadsorbed in the solution was determined by microwave plasma-atomic emission spectrometry (MP-AES, Agilent Tech. 4200 model, Santa Clara, US).

Each test was repeated at least 3 times, and mean values were used. From MP-AES measurements, the amount of Cr(VI) adsorbed per gram of CCs-AC was calculated with the help of Equation (1).

$$Qe = \frac{(Co - Ce) \cdot V}{m} \qquad (1)$$

Percent adsorption values were also calculated with the help of Equation (2) below.

$$Adsorption\ (\%) = \frac{Co - Ce}{Co} \cdot 100 \qquad (2)$$

Where Co is the initial Cr(VI) concentration (mg/L), Ce is the Cr(VI) concentration remaining in the solution at equilibrium (mg/L), Qe is the amount of Cr(VI) adsorbed per unit CCs-AC (mg/g), V is the solution volume (L), and m is the amount of CCs-AC (g).

3. Results and discussion

3.1. Effect of pH on the adsorption of Cr(VI) ions from aqueous solution onto CCs-AC

In adsorption studies, the pH of adsorbate solutions is extremely important in terms of adsorbent capacity. A series of Cr(VI) solutions with a concentration of 100 mg/L and the pH values adjusted between 2 and 8 were prepared and 10 mL of these solutions were placed in 15 mL polypropylene tubes. 0.05 g CCs-AC was added to these solutions (5.0 g/L suspension), the tubes were capped and shaken for 12 hours. The suspensions were filtered by vacuum filtration and the supernatants were analyzed by MP-AES. The concentrations remaining in the supernatants were subtracted from the initial concentration (100 mg/L) and the percent adsorption values were calculated with the relevant formulas.

Fig. 2 reflects the performance of CCs-AC with varying pH. In parallel with many studies in the literature, Cr(VI) adsorption onto CCs-AC is more

favorable at low pH values [21–23]. In fact, it is normal to observe higher yields at lower pHs because Cr(VI) is present in anionic forms in aqueous solution. Between $1.0 < pH < 3.0$ the predominant form for Cr(VI) is $HCrO_4^-$, while at pH > 6.0 it is CrO_4^{2-}. As a result, whether the medium is acidic or basic, Cr(VI) is always in the anionic form. At low pHs, the surface of the adsorbent is positive due to the abundance of protons and therefore strong electrostatic interactions occur between Cr(VI) in anionic form and CCs-AC. Thus, the adsorption efficiency is quite high at low pHs. As a result, the adsorption efficiency is quite high at low pHs. As the solution pH increases, the net charge of the CCs-AC surface becomes negative, while Cr(VI) is still in negative form. Thus, the adsorption efficiency will gradually decrease due to electrostatic repulsions [24,25].

As it was clear from the pH screening that the optimum solution pH was 2.0, the following studies were carried out at this pH value.

3.2. Effect of contact time on the adsorption of Cr(VI) ions from aqueous solution onto CCs-AC and adsorption kinetics

The systems in which the adsorption mechanism is studied as a function of time are called adsorption kinetics. A 250 mL volume of Cr(VI) solution adjusted to pH 2.0 and 1.25 g CCs-AC (5.0 g/L suspension) were treated for 12 hours. The concentrations of the micropipetted aliquots at certain time intervals during the treatment were measured by MP-AES. The measured concentrations were subtracted from the initial Cr(VI) concentration and the amount of Cr(VI) adsorbed per unit adsorbent (Qt, mg/g) was calculated with the relevant formulas.
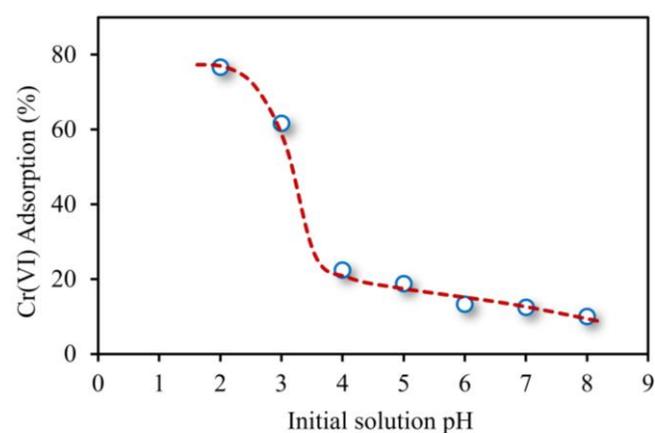
Figure 2. Effect of solution pH on the adsorption of Cr(VI) ions onto CCs-AC from aqueous solution (Co: 100.0 mg/L; Agitation time: 12 h; CCs-AC dosage: 5.0 g/L; CCs-AC particle size: ≤ 125 μm; temperature: 25 °C)

Fig. 3 (a) illustrates the amount of Cr(VI) adsorbed on CCs-AC at different time periods. It is seen that the adsorption is quite fast in the first minutes of the process and the system reaches equilibrium after 2 hours.
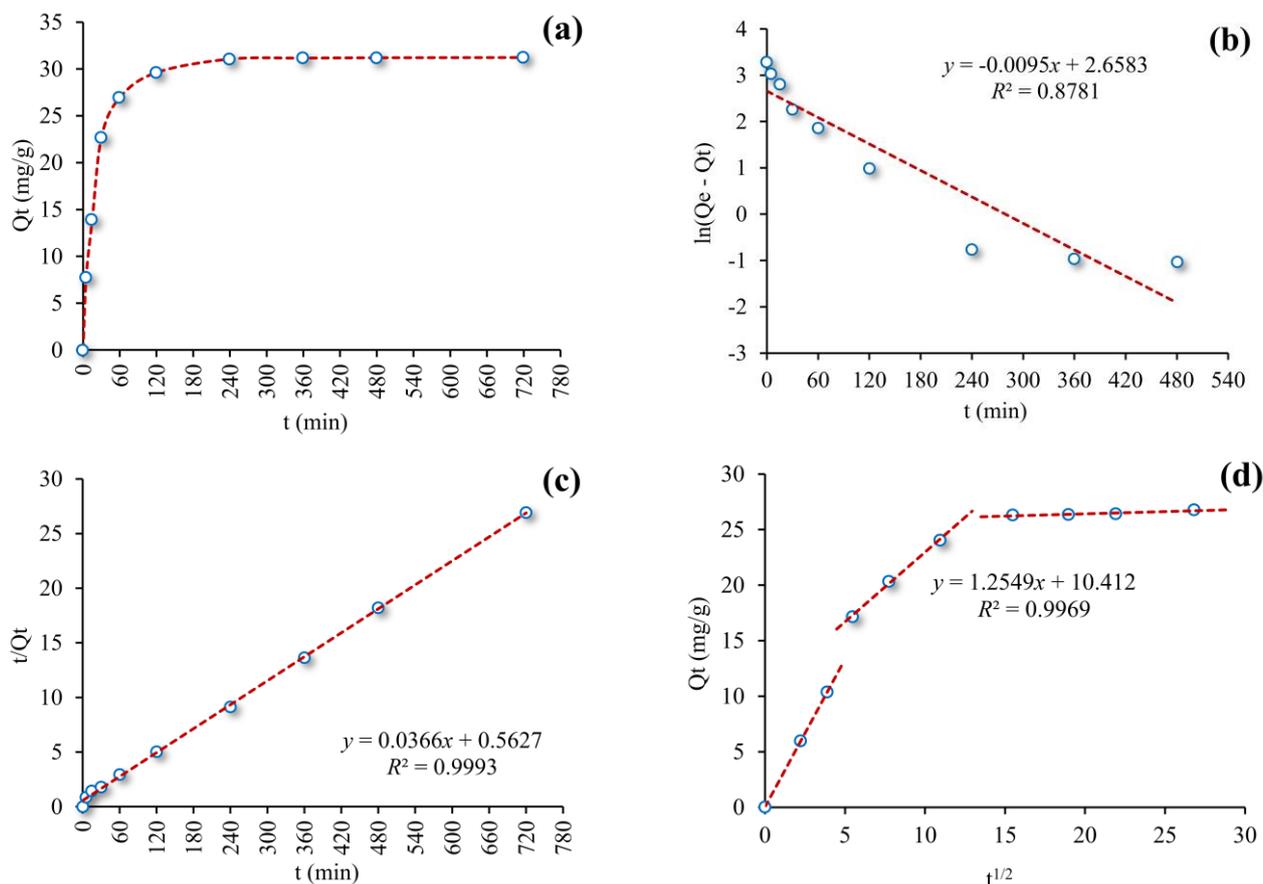
Figure 3. Contact time and adsorption kinetics of Cr(VI) ions onto CCs-AC: (a) Contact time; t vs Qt graph, (b) Pseudo first-order kinetics; t vs ln(Qe – Qt) graph, (c) Pseudo second-order kinetics; t vs t/Qt graph, (d) intraparticle diffusion kinetics; $t^{1/2}$ vs Qt graph (Initial solution pH: 2.0; agitation time: 0–12 h; Co: 250.0 mg/L; CCs-AC dosage: 5.0 g/L)

However, an optimum contact time of 4.0 hours was deemed appropriate as a guarantee.

The behavior of Cr(VI) ions onto CCs-AC in terms of time dependence of adsorption was monitored by pseudo-first order, pseudo-second order and intraparticle diffusion kinetic models. The constants obtained from the relevant equations of these models are given in Table 1.

The mathematical equations of the pseudo-first order kinetic model is shown in Equation (3) and Equation (4). The second equation is a rearrangement and linearization of the first equation.

$$\frac{dQ}{dt} = k_1(Qe - Qt) \qquad (3)$$

$$ln(Qe - Qt) = ln(Qe) - k_1 t \qquad (4)$$

Where Qe represents the amount of adsorbed material per gram of adsorbent at equilibrium (mg/g), Qt represents the amount of adsorbed material per gram of adsorbent at any time t (mg/g), k_1 represents the first order rate constant (1/min) and t represents the contact time (min). The plot of ln(Qe–Qt) versus t forms a line and gives information about the fit of this kinetic model to the adsorption data. Qe and k_1 can be found from the intercept and slope of the graph [26].

Equations for the curvilinear and linear forms of the pseudo-second-order kinetic model, another model used to describe the time dependence of the adsorption process from aqueous solution, are shown in Equation (5) and Equation (6).

$$\frac{dQt}{dt} = k_2(Qe - Qt)^2 \qquad (5)$$

Table 1. Kinetic data for adsorption of Cr(VI) ions from aqueous solution onto CCs-AC

Kinetic models	Constants	Value
	Qe (exp), mg/g	26.75
	Qe (cal), mg/g	14.27
Pseudo first-order	k_1, 1/min	0.00952
	R^2	0.8781
	Qe (exp), mg/g	27.35
Pseudo-second order	k_2, g/mg.min	0.00238
	R^2	0.9993
	k_{id}, mg/g.min$^{1/2}$	1.255
Intraparticle diffusion	C, mg/g	10.41
	R^2	0.9969

$$\frac{t}{Qt} = \frac{1}{k_2 Qe^2} + \frac{t}{Qe} \qquad (6)$$

Where k_2 represents the second order rate constant (g/mg.min). The graph plotted between t/Qt – t forms a line, which shows the agreement of the kinetic data with the second-order kinetic model. Qe and k_2 can be determined from the slope and intercept of the line [27,28].

Fig. 3(b) shows that the adsorption kinetics is not compatible with the pseudo-first order kinetic model ($R^2 = 0.8781$). While this model gives better results for systems that have not yet reached equilibrium, it is insufficient to explain the adsorption rate of systems that can be saturated on porous structures such as activated carbon. This conclusion is also supported by the fact that the experimental Qe value (26.75 mg/g) does not coincide with the theoretical Qe value (14.27 mg/g) obtained from the pseudo-first order (Table 1).

The time-dependent adsorption of various pollutant species from the liquid phase on activated carbon and similar adsorbents gradually slows down and reaches equilibrium when saturation is reached within the capacity of the adsorbent. The adsorption rates of such equilibrium systems are in full agreement with the pseudo-second order kinetic model (Fig. 3(c); $R^2 = 0.9993$). In addition, the experimental Qe value and the theoretical Qe value obtained from this model are very close to each other (Table 1) [29].

In cases where the diffusion mechanism in porous structures cannot be clearly explained by pseudo-first and pseudo-second order equations or when these equations are insufficient, the intraparticle diffusion model may be preferred. This model is given by Equation (7) below.

$$Qt = k_{id}t^{1/2} + C \qquad (7)$$

Where k_{id} (mg/g.min$^{1/2}$) is the intraparticle diffusion rate constant while C (mg/g) is a constant characterizing the boundary layer thickness. k_{id} and C can be determined from the slope and intercept of the graph plotted between Qt and $t^{1/2}$ [26,27].

In the intraparticle diffusion model, the time-dependent stages of adsorption can be estimated. Fig. 3(d) shows that adsorption takes place mainly in 3 stages. The fact that the adsorption rate is very high at the beginning indicates that the outer surface of the activated carbon, i.e. the film layer, is filled first. The second part is slower and here there is a movement of adsorbate ions into the pore interior. This movement is the rate-limiting step of adsorption and indicates the diffusion of adsorbate molecules into the pore interior. The last step is the equilibrium step where adsorption

reaches saturation. For the intraparticle diffusion model, the $t^{1/2}$–Qt plot contains three lines with different slopes as shown in Fig. 3(d). This indicates that more than one process affects adsorption. The second line represents intraparticle diffusion. The C value found for the second line is different from zero (10.41 mg/g), suggesting that the adsorption rate is controlled by other mechanisms besides intraparticle diffusion [26,27].

3.3. Effect of adsorbent dose on the adsorption of Cr(VI) ions onto CCs-AC

In this parameter, it was investigated whether the amount of Cr(VI) adsorbed is linear with increasing amount of CCs-AC. Fig. 4 proves that this relationship is non-linear. The figure illustrates that the amount of Cr(VI) adsorbed per unit adsorbent decreases as the dose of CCs-AC increases due to a non-linear increase in the amount of Cr(VI) adsorbed. Therefore, in the light of these results, it is seen that the lowest CCs-AC dose (1.0 g/L) has the highest Cr(VI) adsorption capacity per unit adsorbent. This inverse relationship can be attributed to two reasons: (*i*) Increasing CCs-AC dose at constant Cr(VI) concentration in solution leads to the formation of unsaturated sites on the adsorbent surface. (*ii*) Agglomeration of CCs-AC particles at high dose leads to a decrease in the total surface area [30,31].

3.4. Effect of initial Cr(VI) concentration on the adsorption efficiency and adsorption isotherms

Increasing adsorbate concentration in aqueous solution at constant adsorbent dose will of course gradually increase the adsorption efficiency. However, as stated in the previous parameter, this increase will not be linear. As the adsorbate gradually reaches saturation, its capacity against the adsorbate of interest will be revealed. This parameter was applied to reveal the adsorption capacity of CCs-AC against Cr(VI) ions from aqueous solution.
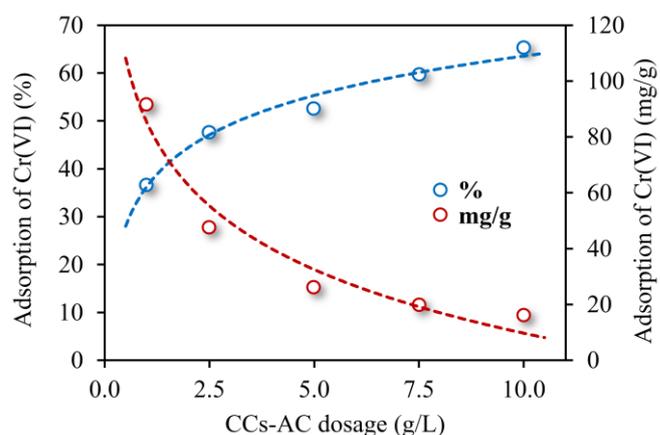
Figure 4. Effect of CCs-AC dosage on the adsorption of Cr(VI) ions onto CCs-AC from aqueous solution (Initial solution pH: 2.0; Co: 250.0 mg/L; agitation time: 4 h; CCs-AC dosage: 1.0–10.0 g/L; CCs-AC particle size: ≤ 125 μm; temperature: 25 °C)
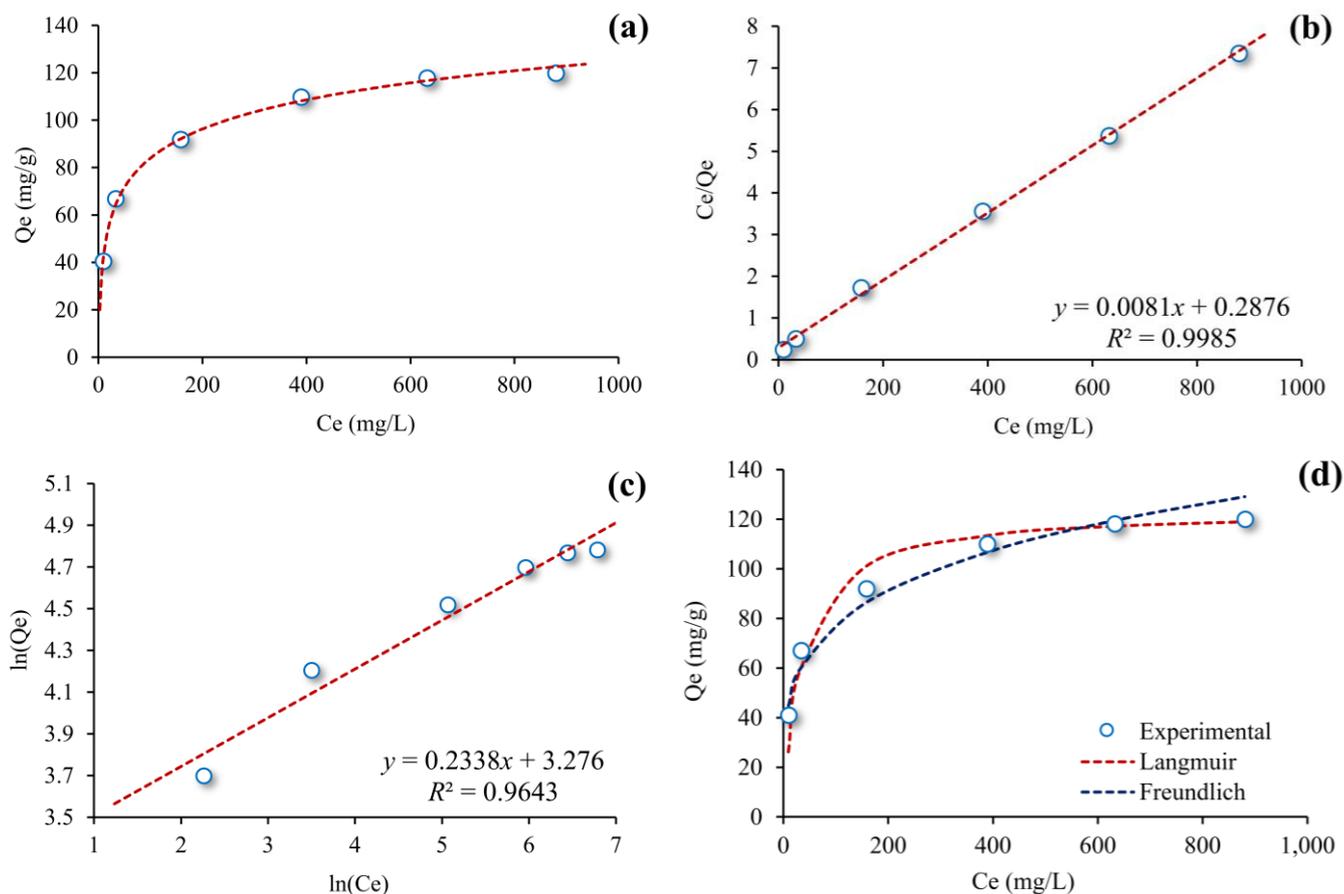
Figure 5. Concentration effect on the adsorption of Cr(VI) ions onto CCs-AC and the adsorption isotherms: (a) Ce – Qe graph, (b) Ce – Ce/Qe graph for Linear Langmuir isotherm, (c) ln(Ce) – ln(Qe) graph for Linear Freundlich isotherm, (d) Ce – Qe graph for non-linear Langmuir and Freundlich isotherms (Initial solution pH: 2.0; Co: 50–1000 mg/L; agitation time: 4 h; CCs-AC dosage: 1.0 g/L; CCS-AC particle size: ≤ 125 µm; temperature: 25 °C)

The relationship between the adsorbate concentration remaining in the aqueous solution as a result of the adsorption process and the amount of adsorbate adsorbed per unit adsorbent is called adsorption isotherm.

Fig. 5(a) illustrates this relationship. As can be seen from the figure, the amount of Cr(VI) adsorbed per unit CCs-AC (mg/g) increases non-linearly with increasing initial Cr(VI) concentration in aqueous solution. The part of the graph where the adsorption reaches maximum saturation indicates the capacity of CCs-AC.

Langmuir and Freundlich isotherm models are more preferred than others in adsorption studies from aqueous solution. The Langmuir model is successfully applied to monolayer systems on homogeneous surfaces and to systems where relatively active sites have equal energy. The capacities of adsorbents that can comply with these conditions can be determined quite accurately with this model [29].

Langmuir adsorption model is given by Equation (8) below:

$$Qe = \frac{bCe}{1 + bCe} \tag{8}$$

Equation (8) can be modified to derive its linear form in Equation (9):

$$\frac{Ce}{Qe} = \frac{Ce}{Q_{max}} + \frac{1}{bQ_{max}} \tag{9}$$

Where Ce is the concentration of adsorbate remaining unadsorbed in solution (mg/L), Qe is the amount of adsorbate adsorbed per unit adsorbent (mg/g), Q_{max} is the maximum adsorption capacity (mg/g) and b is the constant related to the free energy or enthalpy of adsorption (L/mg).

The plot of Ce versus Ce/Qe forms a line and indicates whether the adsorption follows the Langmuir model. Q_{max} and b can be determined from the slope and the intercept, respectively. Q_{max} will give the maximum adsorption capacity of the adsorbent of interest [32,33].

R_L, an important parameter of Langmuir isotherm, indicates whether the selected adsorbent-adsorbate relationship is suitable for adsorption. R_L is a dimensionless constant and is also called the separation factor or equilibrium parameter. R_L is expressed by Equation (10).

$$R_L = \frac{1}{1 + bCo} \qquad (10)$$

Where Co is the initial adsorbate concentration (mg/L). b is a constant (L/mg) derived from the Langmuir equation. The RL value calculated from the formula is expected to be between 0 and 1 for the suitability of adsorption. In cases where R_L is greater than 1, it indicates that adsorption is not suitable for the selected adsorbent-adsorbate pair. When the R_L value is exactly equal to 1, it indicates that the adsorption is linear and when R_L is 0, it indicates that the adsorption is irreversible [7,15,29].

The other type of isotherm, Freundlich isotherm, is related to monolayer/multilayer adsorption from aqueous solution on heterogeneous surfaces. The mathematical expression of this model is as in Equation (11).

$$Qe = K_f \times Ce^{1/n} \qquad (11)$$

For simplicity of calculations in adsorption studies Equation (11) is usually used by taking the logarithm of both sides of the equation and transforming it into linear form (Equation 12).

$$ln(Qe) = ln(K_f) + \frac{1}{n} ln(Ce) \qquad (12)$$

Where K_f (mg/g) and n are constants of this model and are related to adsorption capacity and adsorption density, respectively [32,33].

In this parameter, a series of Cr(VI) solutions prepared between 50–1000 mg/L and CCs-AC at a dose of 1.0 g/L were treated under optimum conditions. The Cr(VI) concentration remaining in the solution (Ce) after filtration and the amount of Cr(VI) adsorbed per gram of CCs-AC (Qe) were calculated with the help of the relevant equations. Firstly, the graph in Fig. 4(a) was plotted as mentioned above. Then the linear graphs of Langmuir and Freundlich adsorption isotherms in Fig. 5(b) and Fig. 5(c) were plotted from the relevant linear formulas, respectively. The constants obtained from these graphs are given in Table 2.

As can be seen from Table 2, Fig. 5(b) and Fig. 5(c), the correlation coefficient for the linear Langmuir isotherm is larger than that obtained from the Freundlich isotherm. Therefore, it can be considered that

the experimental data are more compatible with the Langmuir model. However, in order to reach this conclusion definitively, the curvilinear forms of the related isotherm models should be compared. For this purpose, the constants obtained from the linear equations in Equation (9) and Equation (12) were used in the curvilinear equations Equation (8) and Equation (11) to theoretically re-derive the Qe values. When these theoretical Qe values and experimental Qe values are shown on the same graph in Fig. 5(d), it can be said that the theoretical Qe values that best represent the experimental Qe values are mostly obtained from the Freundlich isotherm model. However, unlike the linear forms, no definite conclusion could be reached here. The adsorption behavior is more in agreement with the Freundlich model at relatively small concentrations and with the Langmuir model at high concentrations.

The Cr(VI) capacity value (Q_{max} = 123.7 mg/g) derived by taking the inverse of the slope in the linear graph of the Langmuir isotherm model can be considered as quite high compared to the literature (Table 3). R_L values, another Langmuir parameter, were also calculated with the help of Equation (10). R_L values calculated for Co values between 50–1000 mg/L were found to be 0.42–0.03. This result shows the suitability of Cr(VI) adsorption onto CCs-AC.

3.5. Desorption of Cr(VI) ions adsorbed on CCs-AC

Desorption of adsorbate ions or molecules retained onto an adsorbent, in other words regeneration of the adsorbent used, is extremely important for the economy and usability of the system. Since Cr(VI) ions are in anionic form in solution at all pHs, they are adsorbed with much higher performance in the acidic region. Therefore, desorption efficiency will be very low with acidic characterized desorption solutions. As seen in the

Table 3. Comparison of Cr(VI) adsorption capacity of various activated carbon-based adsorbents

Precursor	Activating agent	Adsorbent dosage (g/L)	Q_{max} (mg/g)	Reference
Rice husk	$ZnCl_2$	2.0	56.82	[15]
Olive bagasse	Steam	2.0	109.89	[22]
Pomegranate husk	H_2SO_4	2.0	35.2	[23]
Corn cob	CO_2	5.0	57.37	[42]
Commercial AC	SiO_2	1.0	60.9	[43]
Corn cob	$ZnCl_2$–NH_4Cl	0.5	34.48	[44]
Fir wood	KOH	0.4	180.3	[45]
Hazelnut shell	H_2SO_4	2.5	170.0	[46]
Coconut shell	Chitosan	1.0	64.49	[47]
Aloe vera leaves	HNO_3	2.0	59.88	[48]
Corn cob	H_3BO_3	1.0	123.7	This work

pH study, the adsorption efficiency of Cr(VI) ions in the basic region is very low. Therefore, a series of NaOH solutions were prepared at concentrations between 0–3 mol/L for the desorption of Cr(VI) ions adsorbed onto CCs-AC.

Table 2. Langmuir and Freundlich constants for Cr(VI) ions

Langmuir constants				Freundlich constants		
Q_{max} (mg/g)	Q_{max} (mmol/g)	b (L/mg)	R^2	K_f (mg/g)	n	R^2
123.7	2.38	0.0281	0.9985	26.47	4.28	0.9643

CCs-AC at a dose of 5.0 g/L was placed in a series of polypropylene tubes. After adding 100 mg/L Cr(VI) solutions, they were shaken under optimum conditions. After filtration, the CCs-ACs in the tubes were air dried and then a series of NaOH solutions in the range of 0–3 M were added separately, and the desorption was carried out for 4 hours. The Cr(VI) concentrations desorbed into the solution were measured by MP-AES and after necessary calculations, Fig. 6 was plotted.

The results from Fig. 6 show that even the most concentrated NaOH solution (3.0 M) could not quantitatively desorb Cr(VI) ions adsorbed onto CCs-AC. This result proves that unlike typical cationic metal ions, Cr(VI) ions are much more strongly adsorbed onto CCs-AC. Since cationic metal ions bind to functional groups on many adsorbents by weak electrostatic interactions, their desorption can be achieved quantitatively even with very weakly acidic solutions. Cr(VI) ions, which are present in aqueous solution at relatively low pHs, mostly in the form of $HCrO_4^-$, bind to the adsorbent with much stronger interactions, especially chemically. Studies supporting this result are found in the literature [34–38].

3.6. Effect of temperature on the adsorption of Cr(VI) ions onto CCs-AC and adsorption thermodynamics

Temperature is an important indicator of whether the system works under all conditions, how well it performs under which ambient conditions, in short, how close its performance is to laboratory conditions in real applications. In addition, the study of temperature changes is an important parameter that is frequently applied in understanding the mechanism and energy of adsorption.

For this purpose, 5.0 g/L CCs-AC and a series of 250 mg/L Cr(VI) solutions were treated separately at temperatures ranging from 5–50 °C. The concentrations of Cr(VI) remaining unadsorbed in the solution after filtration were determined by MP-AES, from which the amount of Cr(VI) loaded per gram of adsorbent (mg/g) was calculated.

The temperature vs Qe plot is given in Fig. 7(a). As can be seen from the figure, the adsorption behavior of Cr(VI) ions onto CCs-AC is via endothermic mechanism, that is, the increase in ambient temperature positively affects the adsorption efficiency.

The absorption and diffusion of energy during all kinds of events and chemical reactions, the transformation of one type of energy into another type and the relations between different types of energy in a system are the subject of thermodynamics. Thermodynamics determines the internal energy, enthalpy, entropy, and free energy values of the system during a physical or chemical transformation and examines their dependence on the reaction conditions.
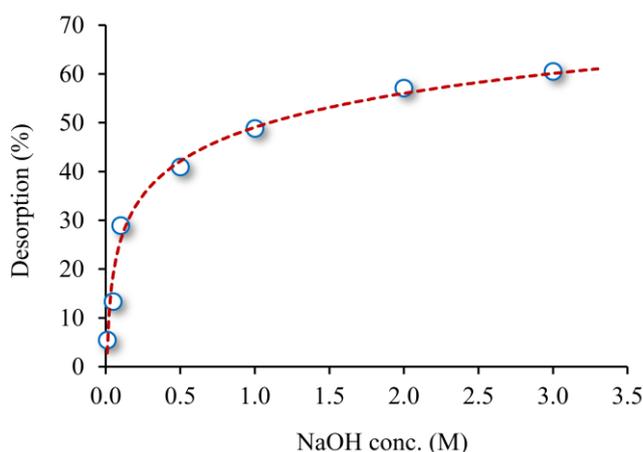
Figure 6. Desorption of Cr(VI) ions adsorbed on CCs-AC (Co: 100 mg/L)
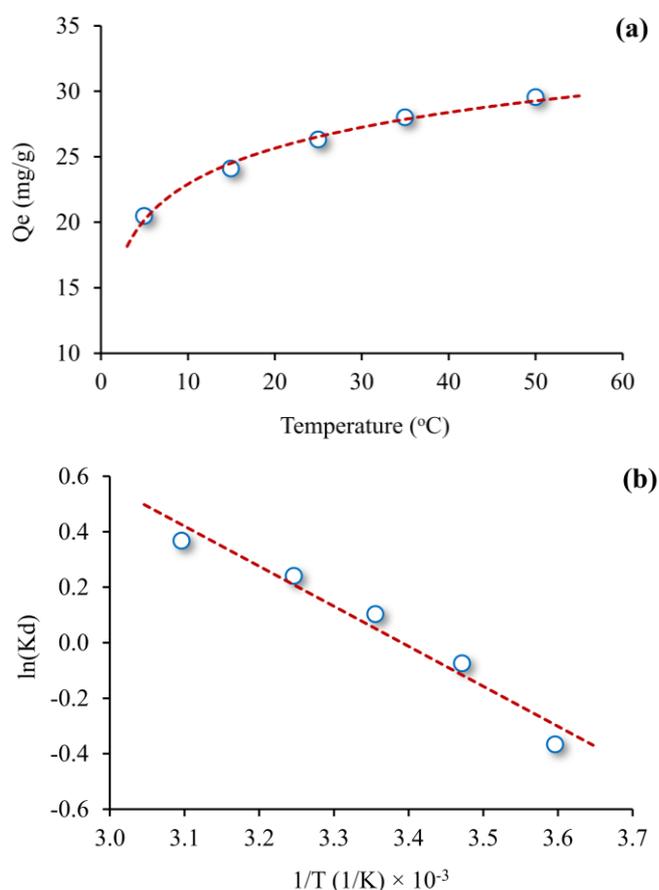
Figure 7. Effect of temperature on adsorption of Cr(VI) ions onto CCs-AC and thermodynamics: (a) Temp. – Qe graph, (b) 1/T – ln(Kd) graph for thermodynamic parameters (Co: 250 mg/L; pH: 2.0; CCs-AC dosage: 5.0 g/L; agitation time: 4 h; CCs-AC particle size: ≤ 125 μm; temperature: 5–50 °C)

The sum of all kinds of energy that a substance stores in its structure is called enthalpy (H). In chemical reactions, the difference between the sum of the enthalpies of the products and the sum of the enthalpies of the reactants is called the enthalpy of reaction (ΔH). Entropy (ΔS) is the energy that cannot be converted into work in a physical system. The Gibbs free energy change (ΔG) is used to express the equilibrium state and willingness of a system. In spontaneous chemical

reactions and other physicochemical transformations, the free energy decreases, so the standard ΔG becomes negative. In short, for any system, all the energy is expressed by enthalpy (H), the available energy by free energy (G) and the unavailable energy by entropy (S). The equations derived for these concepts related to thermodynamics are given in Equations 13–16.

$$\Delta G = \Delta H - T\Delta S \qquad (13)$$

$$\Delta G = -RT ln(K_d) \qquad (14)$$

$$K_d = \frac{Ca}{Ce} \qquad (15)$$

$$ln(K_d) = \frac{\Delta S}{R} - \frac{\Delta H}{RT} \qquad (16)$$

Where T is the temperature (K), R is the gas constant (8.314 J/mol.K), K_d is the adsorption equilibrium constant, Ca is the concentration of adsorbate retained onto the adsorbent (mg/L), Ce is the adsorbate concentration remaining in the solution after adsorption (mg/L).

The graph of $ln(K_d)$ vs 1/T forms a line (Fig. 7(b)) . From the slope of this line ΔH and from the intercept ΔS can be found (Table 4), thus providing information about the reaction course.

The ΔG values in Table 4 become more negative in parallel with the increase in temperature. This indicates that adsorption occurs spontaneously. In cases where the adsorption efficiency is below 50%, $ln(K_d)$ values are negative and therefore ΔG values are positive. As the adsorption efficiency increases above 50% with increasing temperature, $ln(K_d)$ values are also positive. As a result, ΔG values will be negative.

The decrease in ΔG values with increasing temperature increases the feasibility of adsorption and the possibility of spontaneous formation. For the selected initial Cr(VI) concentration (250 mg/L), the feasibility of adsorption becomes more feasible at higher temperatures. Therefore, it is more important that ΔG decreases in relative value with increasing temperature rather than being positive or negative. This is not the case for low

Cr(VI) concentrations. At low Cr(VI) concentrations, room temperature is sufficient for the spontaneous formation of adsorption.

A positive ΔH value indicates that the adsorption of Cr(VI) ions onto CCs-AC is endothermic. The ΔH value can also help to decide whether the adsorption is chemical or physical. The enthalpy value of physical adsorption is generally not greater than 4 kJ/mol and for chemical adsorption not less than 20 kJ/mol [39,40]. The ΔH value is 12.0 kJ/mol (Table 4), which means that the adsorption of Cr(VI) ions on CCs-AC is slightly chemical rather than physical. Quantitative regeneration did not occur in the desorption study anyway.

A positive ΔS value (40.69 J/mol.K) increases the probability of randomization of the adsorption equilibrium occurring at the solid-liquid interface of the adsorbent during adsorption. In other words, this value indicates an increase in the amount of unused energy, i.e. an increase in the disorder of the system [41].

4. Conclusion

The data obtained from this study showed that activated carbon (CCs-AC) produced by chemical activation using boric acid from corn cobs, an agricultural waste by-product, can effectively remove Cr(VI) ions from aqueous solution. Moreover, with an adsorption capacity of 123.7 mg/g Cr(VI), CCs-AC has an even higher capacity than the activated carbons used in many studies in the literature.

As a result of optimization studies with model Cr(VI) solutions, it was determined that the optimum pH was 2.0 and the contact time was 4.0 hours. From the kinetic data, it was concluded that Cr(VI) adsorption on CCs-AC was consistent with the pseudo-second order kinetic model and the adsorption rate was controlled by the boundary layer diffusion together with the intraparticle diffusion.

From the thermodynamic data, it was determined that temperature had a positive effect on adsorption, thus, from the enthalpy value of 12.0 kj/mol, the reaction was endothermic, and the adsorption process was rather chemically driven. The negative Gibs free energy values proved that the adsorption was spontaneous.

This study is important in several ways: (*i*) Activated carbon was produced from corn cobs, an agricultural waste that is not used for any purpose, giving them an economic value. (*ii*) Possible damage to the environment from these wastes discharged into the environment was prevented. (*iii*) Recycling activities were encouraged by recycling wastes that have no economic value.

Table 4. Thermodynamic data for adsorption of Cr(VI) ions from aqueous solution onto CCs-AC

T (°C)	K_d	ΔG (kj/mol)	ΔS (J/mol.K)	ΔH (kj/mol)
5	0.69	0.85		
15	0.93	0.18		
25	1.11	-0.26	40.69	12.00
35	1.27	-0.62		
50	1.44	-1.85		

Acknowledgements

References

[1] Y. Wang, C. Peng, E. Padilla-Ortega, A. Robledo-Cabrera, A. López-Valdivieso, Cr(VI) adsorption on activated carbon: Mechanisms, modeling and limitations in water treatment, J Environ Chem Eng, 8(4), 2020, 104031.

[2] S. Sujatha, R. Sivarethinamohan, A critical review of Cr(VI) ion effect on mankind and its amputation through adsorption by activated carbon, Materials Today: Proceedings, 37(2), 2021, 1158–1162.

[3] WHO, Guidelines for Drinking-water Quality, Fourth edition incorporating the first addendum, WHO Headquarters in Geneva, 2017.

[4] R.C. Bansal, M. Goyal, Activated carbon adsorption, 2005, CRC Press, London, UK, Taylor and Francis.

[5] Z.E. Sayın, C. Kumaş, B. Ergül, Activated carbon production from hazelnut shells (in Turkish), AKU J Sci Eng, 16, 2016, 025805(409–419).

[6] C. Djilani, R. Zaghdoudi, F. Djazi, B. Bouchekima, A. Lallam, A. Modarressi, M. Rogalski, Adsorption of dyes on activated carbon prepared from apricot stones and commercial activated carbon, J Taiwan Inst Chem E, 53, 2015, 112–121.

[7] M. Abbas, S. Kaddour, M. Trari, Kinetic and equilibrium studies of cobalt adsorption on apricot stone activated carbon, J Ind Eng Chem, 20(3), 2014, 745–751.

[8] M. Koohestani, A. Salem, S. Salem, Decolorization of corn syrup in a dynamic system by activated carbon bed: Microwave-assisted impregnation of H_3PO_4 over cherry and date stones for efficient purification, Sustain Chem Pharm, 36, 2023, 101298.

[9] A.C. Lua, J. Guo, Preparation and characterization of activated carbons from oil-palm stones for gas-phase adsorption, Colloid Surface A, 179(2–3), 2001, 151–162.

[10] J. Serafin, B. Dziejarski, J. Sreńsek-Nazzal, An innovative and environmentally friendly bioorganic synthesis of activated carbon based on olive stones and its potential application for CO_2 capture, Sustain Mater Technol, 38, 2023, e00717.

[11] I. Okman, S. Karagöz, T. Tay, M. Erdem, Activated carbons from grape seeds by chemical activation with potassium carbonate and potassium hydroxide, Appl Surf Sci, 293, 2014, 138–142.

[12] H. Boulika, M.E. Hajam, M.H. Nabih, I.R. Karim, N.I. Kandri, A. Zerouale, Definitive screening design applied to cationic & anionic adsorption dyes on Almond shells activated carbon: Isotherm, kinetic and thermodynamic studies, Materials Today: Proceedings, 72(7), 2023, 3336–3346.

[13] D.S.G.D. Senewirathna, S. Thuraisingam, S. Prabagar, J. Prabagar, Fluoride removal in drinking water using activated carbon prepared from palmyrah (Borassus flabellifer) nut shells, Curr Res Green Sustain Chem, 5, 2022, 100304.

[14] A. Putranto, Z.W. Ng, T. Hadibarata, M. Aziz, J.Y.J. Yeo, S. Ismadji, J. Sunarso, Effects of pyrolysis temperature and impregnation ratio on adsorption kinetics and isotherm of

methylene blue on corn cobs activated carbons, S Afr J Chem Eng, 42, 2022, 91–97.

[15] X. Zhang, S. Wu, Y. Liu, Z. Wang, H. Zhang, R. Xiao, Removal of Cr(VI) from aqueous solution by Rice-husk-based activated carbon prepared by Dual-mode heating method, Carbon Res Conver, 6(2), 2023, 76–84.

[16] E.R. Raut, M.A. Bedmohata, A.R. Chaudhari, Comparative study of preparation and characterization of activated carbon obtained from sugarcane bagasse and rice husk by using H_3PO_4 and $ZnCl_2$, Materials Today: Proceedings, 66(4), 2022, 1875–1884.

[17] P. Paraskeva, D. Kalderis, E. Diamadopoulos, Production of activated carbon from agricultural by-products, J Chem Technol Biotechnol 83(5), 2008, 581–592.

[18] T.M. Alslaibi, I. Abustan, M.A. Ahmad, A.A. Foul, A review: production of activated carbon from agricultural byproducts via conventional and microwave heating, J Chem Technol Biotechnol, 88, 2013, 1183–1190.

[19] A. Gundogdu, P. Bozbeyoglu, M. Imamoglu, C. Baltaci, C. Duran, V.N. Bulut, Characterization of the adsorption mechanism of cadmium(II) and methylene blue upon corncobs activated carbon, Anal Let, 56(3), 2023, 433–448.

[20] A. Sharma, N. Kumar, M. Sillanpää, P.R. Makgwane, S. Kumar, K. Kumari, Carbon nano-structures and functionalized associates: Adsorptive detoxification of organic and inorganic water pollutants, Inorg Chem Commun, 141, 2022, 109579.

[21] C. Duran, D. Ozdes, A. Gundogdu, M. Imamoglu, H.B. Senturk, Tea-industry waste activated carbon, as a novel adsorbent, for separation, preconcentration and speciation of chromium, Anal Chim Acta, 688(1), 2011, 75–83.

[22] H. Demiral, İ. Demiral, F. Tümsek, B. Karabacakoğlu, Adsorption of chromium(VI) from aqueous solution by activated carbon derived from olive bagasse and applicability of different adsorption models, Chem Eng J, 144(2), 2008, 188–196.

[23] A.E. Nemr, Potential of pomegranate husk carbon for Cr(VI) removal from wastewater: Kinetic and isotherm studies, J. Hazard Mater 161(1), 2009, 132–141.

[24] Y. Alvarez-Galvan, B. Minofar, Z. Futera, M. Francoeur, C. Jean-Marius, N. Brehm, C. Yacou, U.J. Jauregui-Haza, S. Gaspard, Adsorption of hexavalent chromium using activated carbon produced from sargassum ssp.: comparison between lab experiments and molecular dynamics simulations, Molecules, 27(18), 2022, 6040.

[25] W. Liu, J. Zhang, C. Zhang, L. Ren, Preparation and evaluation of activated carbon-based iron-containing adsorbents for enhanced Cr(VI) removal: mechanism study, Chem Engin J, 189–190, 2012, 295–302.

[26] H. Qiu, L. Lv, B.c. Pan, Q.j. Zhang, W.m. Zhang, Q.x. Zhang, Critical review in adsorption kinetic models. J. Zhejiang Univ. Sci. A 10, 2009, 716–724.

[27] S. Mandal, J. Calderon, S.B. Marpu, M.A. Omary, S.Q. Shi, Mesoporous activated carbon as a green adsorbent for the removal of heavy metals and Congo red: characterization, adsorption kinetics, and isotherm studies, J Contam Hydrol, 243, 2021, 103869.

[28] J. Wang, X. Guo, Adsorption kinetic models: physical meanings, applications, and solving methods, J Hazard Mater, 390, 2020, 122156.

[29] D. Özdeş, C. Duran, S.T. Ozeken, O. Kalkisim, Y. Top, Natural and H_2SO_4 modified plane sawdust as a low-cost adsorbent: removal of anionic and cationic dyes from aqueous solutions, Turk J Anal Chem, 5(1), 2023, 32–42.

[30] G.B. Adebayo, H.I. Adegoke, S. Fauzeeyat, Adsorption of Cr(VI) ions onto goethite, activated carbon and their composite: kinetic and thermodynamic studies, Appl Wat Sci, 10, 2020, 213.

[31] M.E. Goher, A.M. Hassan, I.A. Abdel-Moniem, A.H. Fahmy, M.H. Abdo, S.M. El-Sayed, Removal of aluminum, iron and manganese ions from industrial wastes using granular activated

carbon and Amberlite IR-120H, Egypt J Aqu Res, 41(2), 2015, 155–164.

[32]   W. Somyanonthanakun, R. Ahmed, V. Krongtong, S. Thongmee, Studies on the adsorption of Pb(II) from aqueous solutions using sugarcane bagasse-based modified activated carbon with nitric acid: kinetic, isotherm and desorption, Chem Physics Impact, 6, 2023, 100181.

[33]   Y. Zhou, J. Lu, Y. Zhou, Y. Liu, Recent advances for dyes removal using novel adsorbents: a review, Environ. Pollut., 252 (2019), 352–365.

[34]   B. Singha, S.K. Das, Biosorption of Cr(VI) ions from aqueous solutions: Kinetics, equilibrium, thermodynamics and desorption studies, Colloid Surface B, 84(1), 2011, 221–232.

[35]   A. Tytłak, P. Oleszczuk, R. Dobrowolski, Sorption and desorption of Cr(VI) ions from water by biochars in different environmental conditions. Environ Sci Pollut Res 22, 2015, 5985–5994.

[36]   E. Daneshvar, M.J. Zarrinmehr, M. Kousha, A.M. Hashtjin, G.D. Saratale, A. Maiti, M. Vithanage, A. Bhatnagar, Hexavalent chromium removal from water by microalgal-based materials: adsorption, desorption and recovery studies, Biores Technol, 293, 2019, 122064.

[37]   J. Bayuo, M.A. Abukari, K.B. Pelig-Ba, Desorption of chromium (VI) and lead (II) ions and regeneration of the exhausted adsorbent. Appl Water Sci, 10, 2020, 171.

[38]   D. Ozdes, A. Gundogdu, B. Kemer, C. Duran, M. Kucuk, M. Soylak, Assessment of kinetics, thermodynamics and equilibrium parameters of Cr(VI) biosorption onto Pinus brutia Ten, Canadian J Chem Eng, 92, 2014, 139–147.

[39]   M. Khormaei, B. Nasernejad, M. Edrisi, T. Eslamzadeh, Copper biosorption from aqueous solutions by sour orange residue, J Hazard Mater, 149, 2007, 269–274.

[40]   P. Bozbeyoglu, C. Duran, C. Baltaci, A. Gundogdu, Adsorption of methylene blue from aqueous solution with sulfuric acid activated corn cobs: equilibrium, kinetics and thermodynamics assessment, Hittite Journal of Science and Engineering, 7(3), 2020, 239–256.

[41]   T. Karthikeyan, S. Rajgopal, L.R. Miranda, Chromium(VI) adsorption from aqueous solution by *Hevea Brasilinesis* sawdust activated carbon, J Hazard Mater, 124(1-3), 2005, 192–199.

[42]   S. Nethaji, A. Sivasamy A.B. Mandal, Preparation and characterization of corn cob activated carbon coated with nano-sized magnetite particles for the removal of Cr (VI), Biores Technol, 134, 2013, 94–100.

[43]   M. Karnib, A. Kabbani, H. Holaila, Z. Olamaa, Heavy metals removal using activated carbon, silica and silica activated carbon composite, Energy Procedia, 50, 2014, 113–120.

[44]   S. Tang, Y. Chen, X. Ruzhen, W. Jiang, Y. Jiang, Preparation of activated carbon from corn cob and its adsorption behavior on Cr(VI) Removal, Water Sci Technol, 73(11), 2016, 2654–2661.

[45]   L. Khezami, R. Capart, Removal of Chromium (VI)   from aqueous solution by activated carbons: kinetic and equilibrium studies, J Hazard Mater, 123, 2005, 223–231.

[46]   M. Kobya, Removal of Cr(VI) from aqueous solutions by adsorption onto hazelnut shell activated carbon: kinetic and equilibrium studies, Biores Technol, 91, 2004, 317–321.

[47]   Y. Liu, H. Shan, Y. Pang, H. Zhan, C. Zeng, Iron modified chitosan/coconut shell activated carbon composite beads for Cr(VI) removal from aqueous solution, Int J Bio Macromol, 224, 2023, 156–169.

[48]   A.K. Prajapati, S. Das, M.K. Mondal, Exhaustive studies on toxic Cr(VI) removal mechanism from aqueous solution using activated carbon of Aloe vera waste leaves, J Molecul Liq, 307, 2020, 112956.